PHYSICAL REVIEW B VOLUME 50, NUMBER 8 15 AUGUST 1994-II

Dynamic magnetoconductance fluctuations and oscillations in mesoscopic wires and rings

D. Z. Liu
Center for Superconductivity Research, Department of Physics, University of Maryland, College Park, Maryland 20742-4111

Ben Yu-Kuang Hu
Department of Physics, University of Maryland, College Park, Maryland 20742-4111
and Mikroelektronik Centret, Bygning 345 Ø, Danmarks Tekniske Universitet, DK-2800 Lyngby, Denmark

C. A. Stafford and S. Das Sarma
Center for Superconductivity Research, Department of Physics, University of Maryland, College Park, Maryland 20742-4111

(Received 24 May 1994)

Using a finite-frequency recursive Green's-function technique, we calculate the dynamic magnetoconductance fluctuations and oscillations in disordered mesoscopic normal-metal systems, incorporating interparticle Coulomb interactions within a self-consistent potential method. In a disorderd metal wire, we observe ergodic behavior in the dynamic conductance fluctuations. At low ω, the real part of the conductance fluctuations is essentially given by the dc universal conductance fluctuations while the imaginary part increases linearly from zero, but for ω greater than the Thouless energy and temperature, the fluctuations decrease as $\omega^{-1/2}$. Similar frequency-dependent behavior is found for the Aharonov-Bohm oscillations in a metal ring. However, the Al'tshuler-Aronov-Spivak oscillations, which predominate at high temperatures or in rings with many channels, are strongly suppressed at high frequencies, leading to interesting crossover effects in the ω dependence of the magnetoconductance oscillations.

Quantum transport in mesoscopic normal-metal systems has been extensively studied both experimentally and theoretically in the last decade.[1–10] Most of the work has focused on interference effects in *static* ($\omega=0$) transport properties, such as universal conductance fluctuations (UCF) of order e^2/h in wires and hc/e-periodic Aharonov-Bohm oscillations in mesoscopic rings. Recently, the pioneering experiment of Pieper and Price[11] on the frequency dependence of the Aharonov-Bohm effect in Ag rings has stimulated renewed interest in the *dynamic* response of mesoscopic systems. Simultaneously, the development of a finite-frequency Landauer-Büttiker formula[12,13] and other theoretical techniques[14] makes possible a more complete theoretical description of ac transport in mesoscopic systems. The dynamic response of mesoscopic systems is of fundamental interest because the frequency introduces another energy scale into the problem which plays a role quite different from temperature, and there are possible device applications, such as a mesoscopic photovoltaic effect device.[15]

In this paper, we present a theoretical investigation of dynamic magnetoconductance fluctuations and oscillations in disordered mesoscopic normal-metal systems, using the recently developed finite-frequency Landauer-Büttiker formalism.[12,13] An advantage of this formalism is that the qualitative frequency dependence can be understood by simple arguments. Furthermore, this method can take into account the internal potential distribution in the sample due to the dynamic response of the system by an approximate self-consistent potential method.[13] Using this technique, we find that the corrections to the conductance due to charging effects are of order e^2/h in diffusive mesoscopic conductors in the frequency range of interest, indicating the importance of interactions for the dynamic response.

We consider the diffusive but phase-coherent transport regime, where the elastic mean-free path is less than the sample length L, but the temperature T is low enough so that the inelastic mean-free path is much larger than L. There are then three important energy scales in the problem: k_BT, $\hbar\omega$, and the Thouless energy E_c. E_c is defined[5] as the energy change necessary for electrons traversing the sample to pick up a phase difference of order unity. For diffusive transport, where the typical path length $S\sim v_FL^2/D$,

$$E_c\simeq hv_F/S\simeq hD/L^2\simeq g_c\Delta E, \tag{1}$$

where D is the diffusion constant, ΔE is the level spacing at E_F, and g_c is the dc conductance (in units of e^2/h). Interesting effects occur due to the interplay of these three energy scales.

We find the following results: (1) In disordered wires at $T=0$, both the real and (for sufficiently large frequencies) imaginary parts of the conductance fluctuations $\delta g(\omega)$ show UCF for $\omega<E_c$, and both fall as $\omega^{-1/2}$ for $\omega\gg E_c$. These fluctuations are ergodic over all frequencies investigated. (2) In disordered metal rings, the hc/e Aharonov-Bohm (AB) conductance oscillations with respect to magnetic field persist to high frequencies, and have a frequency dependence similar to that of the conductance fluctuations. The $hc/2e$ Altshuler-Aronov-Spivak (AAS) oscillations, which predominate at high temperatures or in samples with many channels, show a more rapid decrease with frequency;[3] as a result, the magnetoconductance oscillations may cross over from AAS to AB behavior when the frequency is increased.

Following conventional treatments,[16] we consider the mesoscopic sample as a disordered region which scatters electrons incident from semi-infinite ordered regions (perfect

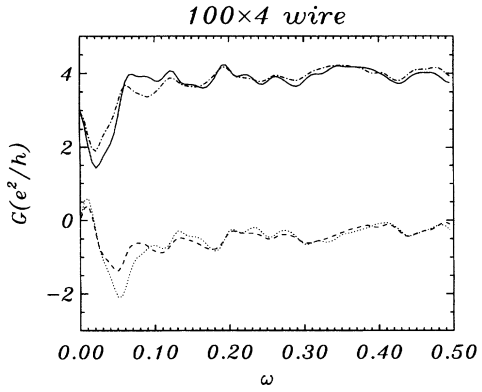

FIG. 1. Dynamic conductance of a 100×4 wire vs frequency ω. Both real (solid line for $C=\infty$, dashed-dot line for $C=0$) and imaginary (dashed line for $C=\infty$, dotted line for $C=0$) parts of the conductance are shown. The disorder amplitude is $W=1$, and E_c is estimated to be 0.03.

"leads"). Using the recently developed finite-frequency Landauer-Büttiker formula, the conductance matrix for a multiprobe system of noninteracting electrons, $g_{\alpha\beta}(\omega) \equiv \langle \delta I_\alpha(\omega)\rangle / \delta U_\beta(\omega)$, where $\langle I_\alpha\rangle$ is the current in lead α and U_β is the potential in lead β, may be written as[12,13]

$$g_{\alpha\beta}(\omega)=\frac{e^2}{h}\int dE\ \mathrm{Tr}\{\mathbf{1}_\alpha\delta_{\alpha\beta}-\mathbf{s}^\dagger_{\alpha\beta}(E)\mathbf{s}_{\alpha\beta}(E+\hbar\omega)\} \times\frac{f(E)-f(E+\hbar\omega)}{\hbar\omega}, \tag{2}$$

where $\mathbf{s}_{\alpha\beta}(E)$ is the scattering matrix for electrons of energy E, and the trace over channels includes spin. Thus the dynamic conductance is related to the correlation of transmission (or reflection) amplitudes at energies differing by $\hbar\omega$. For a mesoscopic conductor with two leads (i.e., $\alpha,\beta=1,2$) there are in general three independent ac response functions;[13] we shall consider the current response in lead 1 due to an ac potential difference applied symmetrically to reservoirs 1 and 2, which for noninteracting electrons is given by $g(\omega)=[g_{11}(\omega)-g_{12}(\omega)]/2$.

We simulate the mesoscopic system using a tight-binding model on a square lattice, with unit nearest-neighbor hopping matrix element. The disorder is modeled by an on-site random potential ranging from $-W/2$ to $W/2$. A magnetic field modifies the hopping term by a Peierls phase factor. The retarded single particle Green's function G^+ is calculated using the recursive Green's-function algorithm.[17,18] For an LM system (length L, width M), the transmission and reflection coefficients $\mathbf{t}\equiv\mathbf{s}_{12}$ and $\mathbf{r}\equiv\mathbf{s}_{11}$ are determined using the following relations:[2]

$$r_{mn}=i(v_m v_n)^{1/2}G^+_{mn}(0,0)-\delta_{mn}, \tag{3a}$$

$$t_{mn}=i(v_m v_n)^{1/2}G^+_{mn}(0,L)e^{ik_n L}, \tag{3b}$$

where $m,n=1,2,\ldots,M$ is the channel number, v_m is the group velocity for channel m, and k_n is the wave vector for channel n. In Fig. 1, we show the real (solid curve) and imaginary (dashed curve) parts of the dynamic conductance of a 100×4 wire versus frequency ω, calculated for noninteracting electrons using Eqs. (2) and (3). This conductance is not current conserving and will be compared with a charge- and current-conserving answer. Figure 1 illustrates the generic frequency dependence of a diffusive metallic conductor: $|\mathrm{Im}[g]|$ increases linearly for small frequencies, becoming comparable to e^2/h when $\omega\sim E_c$; $\mathrm{Re}[g]$ exhibits a weak-localization suppression at low frequencies; both exhibit random fluctuations of order e^2/h on a frequency scale $\sim E_c$, which decrease in amplitude with increasing frequency.

The dynamic response of an *interacting* mesoscopic system depends in detail on the inhomogeneities in the local electric field, which must be determined self-consistently from the external potentials and the dynamic charge distribution in the sample, in contrast to the dc case, where inhomogeneities in the local electric field are irrelevant in linear response. To lowest order, the self-consistent potential due to the interactions in the system can be approximated by a constant induced potential resulting from the charge pileup in the system, $U_0^{\mathrm{ind}}=Q_0/C$, where C is the effective capacitance of the mesoscopic wire or ring. Within this approximation, the response of the interacting system $g^I_{\alpha\beta}$ is charge and current conserving and can be determined from the admittances $g_{\alpha\beta}$ for the noninteracting system as[13]

$$g^I_{\alpha\beta}(\omega)=g_{\alpha\beta}(\omega)-\frac{(i/\omega C)\sum_\gamma g_{\alpha\gamma}(\omega)\sum_\delta g_{\delta\beta}(\omega)}{1+(i/\omega C)\sum_{\gamma\delta} g_{\gamma\delta}(\omega)}. \tag{4}$$

In Fig. 1, the dynamic conductance of the interacting system ($C=0$) is compared to that of the noninteracting system ($C=\infty$). As is evident from Fig. 1, the corrections to the dynamic conductance due to the self-consistent potential are proportional to ω for small frequencies,[13] and are largest in magnitude when $\omega\sim E_c$, where the fluctuations away from zero of the sums over admittances in the second term of Eq. (4) are maximal. The relevant capacitance scale determining the crossover from strongly to weakly interacting behavior is set by the dwell time τ of an electron in the system:[13] if $RC\gg\tau$, interactions can be neglected; if $RC\ll\tau$, interactions enforce charge neutrality. For a typical diffusive mesoscopic conductor, such as the Ag ring of Ref. 11, the RC time is estimated to be several orders of magnitude smaller than the dwell time $\sim h/E_c$, so effectively $C=0$. As shown in Fig. 1, the correction to the conductance due to self-consistent charging effects can be considerable (of order e^2/h). However, we find *no* significant change in the amplitude of the conductance *fluctuations* or *oscillations* when the capacitive effect is incorporated. In the following, averaged quantities shown are for $C=\infty$, while results for a single sample use $C=0$.

Conductance fluctuations similar to those shown as a function of ω in Fig. 1 are obtained when the other parameters of the system are varied. In Fig. 2, we show the dynamic magnetoconductance fluctuations in disordered mesoscopic wires at $T=0$ calculated by averaging over (a) an ensemble of samples, (b) magnetic field, and (c) chemical potential. Regardless of the averaging method, the results

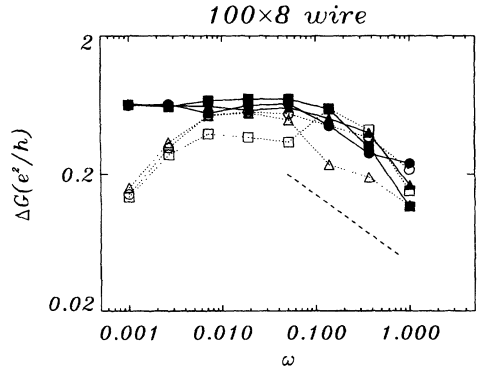

FIG. 2. Frequency dependence of the conductance fluctuations for 100×8 wires. Both real (filled symbols connected by solid line) and imaginary (open symbols connected by dotted line) are shown. Cirles are for 100 sample ensemble average; squares are for magnetic field average ($\alpha=0$–0.1); triangles are for chemical potential avegrage ($\mu=-0.4$–0.4). The dashed line indicates the $\omega^{-1/2}$ behavior. $W=1$ and $E_c\simeq 0.03$.

obtained were equivalent within our statistical uncertainty (see Fig. 2), demonstrating the *ergodicity* of the system. At low frequencies, $\omega \ll E_c$, the root mean square value of the real part of the conductance fluctuations, Re$[\Delta g]$, is given by the UCF value ($\approx 0.6e^2/h$), independent of sample size (as long as the sample is in the quantum coherent transport regime, as we have assumed), while Im$[\Delta g]$ increases linearly and saturates at the same universal value. In the high frequency limit, $\omega \gg E_c$, $\Delta g \sim \omega^{-1/2}$, as shown in Fig. 2. The ω dependence of Δg may be understood by simple qualitative arguments based on Eq. (2): $g_{\alpha\beta}$ is real for $\omega=0$, but the product $s^{\dagger}_{\alpha\beta}(E)s_{\alpha\beta}(E+\hbar\omega)$ (for a single channel) acquires a complex phase of order unity when $\hbar\omega \sim E_c$, so Re$[\Delta g]$ and Im$[\Delta g]$ become comparable at that frequency. For $\hbar\omega \gg E_c$, the product $s^{\dagger}_{\alpha\beta}(E)s_{\alpha\beta}(E+\hbar\omega)$ has an arbitrary complex phase which varies by an amount of order unity when $E \to E+E_c$. Standard random walk arguments applied to the integral in Eq. (2), whose range is roughly from $\mu-\omega$ to μ, then give Re$[\Delta g]$, Im$[\Delta g] \sim (E_c/\omega)^{1/2}$ for $\hbar\omega \gg E_c, k_BT$.

We now consider dynamic magnetotransport in mesoscopic rings. In the dc case, it is well known that a magnetic

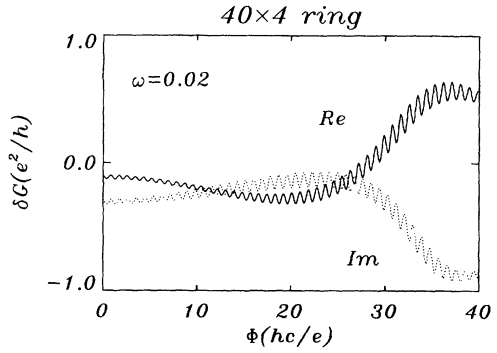

FIG. 3. The Aharonov-Bohm effect for a 40×4 ring at finite frequency ($\omega=0.02\sim E_c$). Here the real part (solid line) is offset by $-4e^2/h$ to compare with the imaginary part (dotted line). The field in the annulus is 25% of that in the hole.

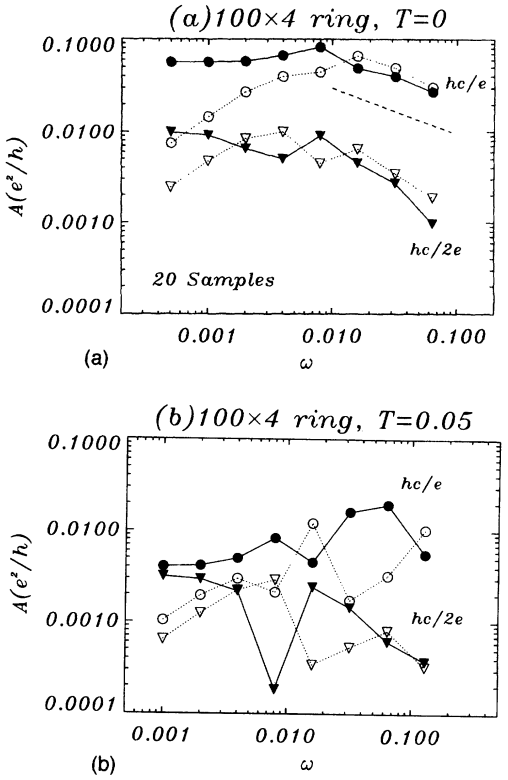

FIG. 4. Frequency dependence of magnetoconductance oscillation amplitudes in mesoscopic rings. $W=1$ and $E_c\simeq 0.01$. The circle is for the AB oscillations, triangle for the AAS oscillations; the solid symbol is for the real part, open symbol for the imaginary part. (a) Zero temperature, 20 sample ensemble average. The dashed line indicates $\omega^{-1/2}$ behavior; (b) $T=0.05$, single sample, $C=0$.

flux placed through a mesoscopic ring generates periodic conductance oscillations with flux period hc/e [the Aharonov-Bohm (AB) effect], and $hc/2e$ [the Al'tshuler-Aronov-Spivak (AAS) effect]. Both have been observed experimentally in mesoscopic rings.[3,5,10] In Fig. 3, we show the calculated conductance oscillations in a mesoscopic ring of circumference 80 with four transverse channels (denoted 40×4) at $\omega \sim E_c$ and $T=0$. For these parameters, the real and imaginary parts of the AB amplitude are comparable, and much greater than the AAS amplitude. The root mean square AB and AAS amplitudes for an ensemble of 20 100×4 rings at $T=0$ are shown in Fig. 4(a). The frequency dependence of the AB amplitude[19] is similar to that of the conductance fluctuations (Fig. 2), while the AAS amplitude is smaller, and has a more rapid decrease with frequency. Qualitatively, this ω dependence may be understood from Eq. (2): The AB effect comes from the quantum interference of electrons going through opposite branches of the ring; since these paths have a random phase difference in zero field even at $\omega=0$, it is not important that $\mathbf{s}_{\alpha\beta}$ and $\mathbf{s}^{\dagger}_{\alpha\beta}$ are evaluated at different energies in Eq. (2) (except that this makes the AB amplitude complex), and the frequency dependence of the AB effect is therefore similar to that of the conductance fluctuations. However, the AAS effect comes from the interference of time-reversed paths encircling the

flux which have equal phases in zero field, so that the AAS effect is insensitive to energy averaging at $\omega=0$. But the finite frequency electric field breaks the time-reversal symmetry of the paths contributing to the AAS effect,[4] leading to an $\omega^{-1/2}\exp[-(\omega/E_c)^{1/2}]$ suppression of AAS oscillations at high frequencies.[3] The different frequency dependence of the AB and AAS amplitudes is particularly evident in Fig. 4(b), which is for a single sample at $T=0.05>E_c$. The finite temperature suppresses the AB effect by energy averaging, but not the AAS effect, so that the two are comparable at $\omega=0$. As the frequency is increased, the AAS effect is strongly suppressed, but the AB effect is not expected to be suppressed until $\omega>k_BT$, and appears to be constant (up to fluctuations) in Fig. 4(b). This crossover from AAS oscillations to AB oscillations demonstrates the qualitatively different role of temperature and frequency in quantum transport in mesoscopic systems.[20] We point out that the ω dependence of the AB effect shown in Fig. 4(b) is consistent with the experimental results in Ref. 11. However, we find that the smallness of Im$[A]$ relative to Re$[A]$ at frequencies greater than E_c is sample specific, and does not persist in the ensemble average [Fig. 4(a)].

In summary, we have calculated the dynamic magnetoconductance for disordered mesoscopic normal metal wires and rings. In a metal wire, we find that the dynamic conductance fluctuations decrease as $(E_c/\omega)^{1/2}$ when the frequency is much larger than the Thouless energy and temperature; at lower frequency, the real part of the conductance fluctuations is essentially given by the dc universal conductance fluctuations while the imaginary part increases linearly from zero. Similar frequency-dependent behavior is found for the hc/e-periodic Aharonov-Bohm oscillation amplitude in a metal ring. For high enough temperatures, we find that the oscillations may cross over from $hc/2e$ period to hc/e period with increasing ω. We find that incorporating interactions through a self-consistent potential changes the magnetoconductance of an individual mesocopic conductor considerably, but does not affect the magnitude of the conductance fluctuations and oscillations.

We acknowledge M. Büttiker for stimulating discussions. We also thank T. Kawamura, J. Pieper, and J. Price for helpful discussions. This work was supported by the National Science Foundation and the U.S. Office of Naval Research.

[1] P. A. Lee, Physica **140A**, 169 (1986); P. A. Lee and A. D. Stone, Phys. Rev. Lett. **55**, 1622 (1985).

[2] A. D. Stone, Phys. Rev. Lett. **54**, 2692 (1985), and references therein.

[3] B. L. Al'tshuler, A. G. Aronov, and B. Z. Spivak, Pis'ma Zh. Eksp. Teor. Fiz. **33**, 101 (1981) [JETP Lett. **33**, 94 (1981)].

[4] B. L. Al'tshuler, A. G. Aronov, and D. E. Khmelnitsky, Solid State Commun. **39**, 619 (1981).

[5] A. D. Stone and Y. Imry, Phys. Rev. Lett. **56**, 189 (1986), and references therein.

[6] M. Büttiker, Phys. Rev. Lett. **57**, 1761 (1986).

[7] H. U. Baranger, A. D. Stone, and D. P. DiVincenzo, Phys. Rev. B **37**, 6521 (1988).

[8] X. C. Xie and S. Das Sarma, Phys. Rev. B **38**, 3529 (1988).

[9] M. Büttiker, Phys. Rev. Lett. **65**, 2901 (1990).

[10] R. A. Webb, S. Washburn, C. P. Umbach, and R. B. Laibowitz, Phys. Rev. Lett. **54**, 2696 (1985).

[11] J. B. Pieper and J. C. Price, Phys. Rev. Lett. **72**, 3586 (1994); Physica B **194/196**, 1051 (1994).

[12] Y. Fu and S. C. Dudley, Phys. Rev. Lett. **70**, 65 (1993).

[13] M. Büttiker, A. Prêtre, and H. Thomas, Phys. Rev. Lett. **70**, 4114 (1993); **71**, 465 (1993); M. Büttiker, H. Thomas, and A. Prêtre, Z. Phys. B **94**, 133 (1994).

[14] Ned S. Wingreen, Antti-Pekka Jauho, and Yigal Meir, Phys. Rev. B **48**, 8487 (1993).

[15] V. Fal'ko, Europhys. Lett. **8**, 785 (1989).

[16] R. Landauer, Philos. Mag. **21**, 863 (1970); D. Fisher and P. A. Lee, Phys. Rev. B **23**, 6851 (1981); P. A. Lee and D. Fisher, Phys. Rev. Lett. **47**, 882 (1981).

[17] S. Das Sarma and Song He, Int. J. Mod. Phys. B **7**, 3375 (1993), and references therein.

[18] A. Mackinnon, J. Phys. C **13**, L1031 (1980); Z. Phys. B **59**, 385 (1985).

[19] A similar frequency dependence for the AB effect was obtained by a different method by J. B. Pieper and J. C. Price (unpublished). However, they did not consider charging effects.

[20] A similar crossover is expected at $T=0$ in a ring with many transverse channels, in which the AAS effect is expected to be dominant at low frequencies.